Huotan Jiedu Tongluo Formula Inhibits Atherosclerotic Vulnerable Plaques Via the Autophagy-NLRP3 Inflammasome Signaling Pathway

Miao Zhang[1], Keying Yu[2], Tenghui Tian[2], Tianxia Sun[3], Yue Deng[2], Rui Shi[2], Dongming Xue[3]

[1]Department of Internal Medicine,Affiliated Hospital of Changchun University of Chinese Medicine, Changchun,Jilin,China
[2]Department of Cardiovascular, Affiliated Hospital of Changchun University of Chinese Medicine, Changchun, Jilin, China
[3]Jilin Ginseng Academy, Changchun University of Chinese Medicine, Changchun, Jilin, China

Introduction. Huotan Jiedu Tongluo Formula (HJTF) has been widely used in the clinic to treat atherosclerotic vulnerable plaques (VP). However, the mechanism of HJTF is not clear.

Objective. This study examine the inhibitory effect and potential mechanisms of HJTF against VP in vivo and vitro experiments.

Materials and Methods. In vivo experiments, given a carotid collar and high-cholesterol diet to establish the ApoE$^{-/-}$ VP model and gave the mice (n=12) HJTF (12.103 g/kg/d) gavaged or Evolocumab Injection (18.2 mg/kg/2w) subcutaneous injection for eight weeks. The Sham group (n=12) and Model group (n=12) were given equivalent volumes of distilled water by gavage. Histological examination of the intimal condition of mouse carotid arteries. ELISA to clarify the expression of inflammatory factors in mouse serum. qRT-PCR and Western blot to clarify NLRP3 inflammasome with autophagy-related indicators in mouse carotid artery tissues. In vitro experiments, applied lipopolysaccharide (LPS) induced inflammatory injury models in RAW 264.7 cells to observe the protective effect of HJTF and its effect on the autophagy-NLRP3 inflammasome signaling pathway in vitro.

Result. HJTF could reduce body weight ($P<0.05$) and blood lipids ($P<0.01$) in mice with VP. HJTF also inhibited intimal hyperplasia ($P<0.001$) and collagen fibril deposition ($P<0.01$) in mice's carotid arteries and reduced the content of MMP-9 ($P<0.001$). HJTF reduced the content of inflammatory factors IL-1β ($P<0.01$) and TNF-α ($P<0.05$) in mice serum and increased the level of autophagy in mice carotid arteries to inhibit the expression of NLRP3 inflammatory vesicles. In vitro experiments demonstrated similar results.

Conclusion. HJTF has the potential to inhibit the VP through the autophagy-NLRP3

inflammasome signaling pathway.

Keywords. atherosclerosis; traditional Chinese medicin; vulnerable plaque; NLRP3 inflammasome; autophagy

1. INTRODUCTION

Atherosclerosis(AS) is the key cause of vascular disease globally (Herrington, Lacey et al. 2016). In some developed countries, the mortality rate caused by atherosclerosis reaches 25% (Moss, An et al. 2019). AS disease is characterized by the formation of atherosclerotic plaques, which are divided into stable and unstable plaques (Urbak, Sandholt et al. 2020). Unstable plaque, also known as vulnerable plaque (VP), is prone to the formation of fibrous cap ulcers, plaque rupture, and intraplaque hemorrhage. It is the basis for adverse cardiovascular events such as angina pectoris and myocardial infarction (Giuliani 2019). Studies have confirmed that VP have thin fibrous caps and large lipids (usually 30% to 40% of the total plaque area) and are rich in inflammatory cells such as macrophages and a small number of smooth muscle cells (Pan, Cai et al. 2021).

Research have shown that the NLRP3 inflammasome can induce various types of AS-associated cells to secrete inflammatory factors to participate in the inflammatory reaction of atherosclerosis (AS) (Hoseini, Sepahvand et al. 2018). During the development of AS, Nod-like receptor protein 3 (NLRP3) couldbe activated by cholesterol crystals, oxidized low-density lipoprotein (ox-LDL), and hemodynamic abnormalities. It can recruit apoptosis-associated spot-like protein (SPECK-like protein, ASC) to start the effector protein cysteine aspartic protein one precursor (pro-caspase-1), forming the NLRP3 protein complex and shearing activated caspase-1, activated caspase-1 enzymes can split and activate IL-1β and IL-18 (Kelley, Jeltema et al. 2019). Several mechanisms have been identified to inhibited NLRP3 inflammasome signaling, among which autophagy can recognize substrates and selectively remove them. Autophagy is a "self-healing" process of the organism. We learned that P62/SQSTM1 is a protein with multiple functional, structural domains, which exist in the cytoplasm as dispersed puncta or aggregates (Lamark, Svenning et al. 2017). It was shown that P62/SQSTM1 is involved in selective autophagy as an essential particular autophagic adaptor protein (Biasizzo and Kopitar-Jerala 2020). A study found that P62 co-localized with LC3 protein and ASC by GFP tagging (Elbialy 2021).

Huotan Jiedu Tongluo Formula (HJTF) is developed from the classical Chinese medicine formula Si Miao Yong An Formula. It is based on Si Miao Yong An Formula with Gansong, Danshen, Gualou, Shuizhi, and Hong Jingtian (See Table 1). It has been shown that HJTF has significant hypolipidemic effects and can treat in-stent restenosis after percutaneous coronary intervention, but its mechanism of action in treating AS VP is unclear (Tian, Yu et al. 2021).

Carotid collar animal model has been applied by many scholars to study atherosclerotic VP (von der Thüsen JH 2001). Apolipoprotein E (ApoE) is a component of blood lipids and is involved in cholesterol transport (Marais 2019). It is responsible for the transport of celiac particles that bind to specific hepatic and peripheral cell receptors and is crucial for the proper metabolism of triglyceride-rich lipoprotein components (Huebbe and Rimbach 2017). Pure-hybrid *ApoE* knockout mice lacked ApoE protein and developed normally but significantly increased plasma total cholesterol levels and spontaneous AS lesions (Li, Safitri et al. 2020). In this study, we used a carotid collar + high-fat diet on *ApoE*$^{-/-}$ mice to establish atherosclerotic VP model and applied lipopolysaccharide (LPS) induced inflammatory injury model in RAW 264.7 cells. The aim is to study the regulatory effect of HJTF on the autophagy-NLRP3 inflammasome signaling pathway in VP. It provides a new pharmacological basis for treating atherosclerotic VP in Chinese medicine.

2. MATERIALS AND METHODS

2.1Materials and Reagents

The Chinese medicines (Table 1) constituting HJTF were provided by the Affiliated Hospital of Changchun University of Chinese Medicine (Chang Chun, China). The voucher specimens were deposited at the Jilin Ginseng Academy, Changchun University of Chinese Medicine. Evolocumab Injection (batch number: 86978217000055) was provided by Amgen (CA, USA). Anti-GAPDH, anti-NLRP3, anti-Caspase-1, anti-ULK1, anti-ATG7, anti-LC3B, anti-P62, and HRP-conjugated anti-rabbit IgG were provided from Sigma (MO, USA). Anti-ASC, anti-Beclin1, anti-MTOR, anti-Phospho-MTOR were purchased from Cell Signaling Technology (Danvers, MA). Antibodies against MMP-9 were purchased from Servicebio Corp (Wuhan, China). TRIzol was purchased from Invitrogen Scientific Bio Inc (Waltham, USA).

2.2 Experimental Drug Preparation.

Previous studies have clarified the main ingredients of the HJTF by HPLC-MS/MS.(Tian et al. 2021). Eight herbs were soaked in deionized water for half an hour in proportion to their size, while animal medicines were soaked for 40-50 minutes. Add ten times the weight of the materials to the water. Boiled the animal medicine for about 20 minutes before adding other herbs, then further decocted the medicine for 30 minutes after combining the other herbs. Subsequently, we collected the medicinal juice, filtered the residue, and repeated the operation 1-2 times. At last, all the drug juices were mixed, strained and concentrated to a density of 1.2103 g/mL and stored at 4°C.

2.3 Animals.

Forty eight 12-week-old SPF male *ApoE*$^{-/-}$ mice body weight (25 ± 5 g), provided by Charles River Co., Ltd. (license number: CNAS L2677), housed in Changchun University of Traditional Chinese Medicine SPF Barrier Animal Experiment Center, at 20-26°C, 40-70% relative humidity, and 12h light-dark cycle. All experiments procedures complied with the Experimental Animal Ethics Committee of Changchun University of Chinese Medicine (No. 2020281).

2.4 Model Establishment and Animal Administration.

Mice were fixed on the animal table and anesthetized by abdominal injection of 40 mg/kg of 1% sodium pentobarbital (Sigma-Aldrich, MO, USA). Perform iodophor disinfection with the neck as the center, lay a hole towel, cut the neck skin longitudinally, and bluntly separate the anterior cervical glands. The pulsating right carotid artery that can be seen pulsating was located on the right side of the trachea. Carefully separate the common carotid artery from the bifurcation. Place a silicone cannula with a length of 2.5mm and an inner diameter of 0.3mm (the outer diameter of the mouse carotid artery is about 0.5mm) on the periphery of the blood vessel. The proximal and distal segments of the cannula are made of thin silk threads (The diagram of the carotid collar operation has shown in Figure1). Fix with ligation. The carotid artery was reset, and the anterior skin of the neck was sutured intermittently. After the restoration of blood flow and confirmation of no bleeding, surgical incision was sutured. Subsequently, given a high-fat diet (0.25% cholesterol and 15% cocoa butter) for eight weeks. The mice in the Sham group cut the neck skin, and the neck skin was sutured directly without cannula.

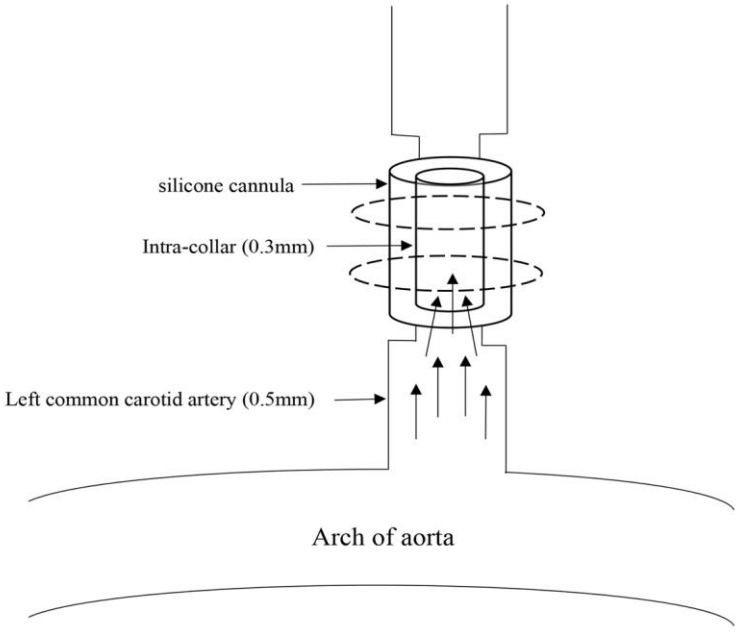

Figure 1. The diagram of the carotid collar operation

The mice were randomized with four groups, namely, the Sham group (Sham+normal diet, n=12), the Model group (Carotid collar+high-fat diet, n=12), HJTF group (Carotid collar+high-fat diet+HJTF, n=12), and Evolocumab group (Carotid collar+high-fat diet+Evolocumab, n=12). The doses of HJTF and Evolocumab were calculated according to the equivalent dose formulas for humans and animals as depicted in the second edition of Experimental Methodology of Pharmacology (1991). The mice in the HJTF group were gavaged HJTF at a dose of 12.103 g/kg/d, and the Evolocumab group was given Evolocumab Injection 18.2 mg/kg/2w subcutaneous injection. Similarly, the Sham and Model group mice were gavaged the same amount of distilled water. After 8 weeks, all mice were fasted for 12 hours and then given anesthesia (sodium 40mg/kg 1%) and sacrificed. The damaged carotid artery of all mouse was collected and fixed with 4% paraformaldehyde.

2.5 Histological examinations.

The carotid arteries were visualized by routine hematoxylin-eosin (H&E) staining. Collagen fibers were stained blue by Masson's stain. The Vascular were fixed in 4% formaldehyde and then paraffin-embedded, and 4-μm-thick tissue sections were cut off for staining and observation. The slides were observed using a Leica light microscope

and the neointima area (NIA) was measured using Image-Pro Plus 6.0 software (Media Cybernetics, USA).

2.6 Immunocytochemical analysis.

Paraffin sections of mice carotid arteries were dewaxed to water. Endogenous peroxidase was removed by adding 3% H_2O_2, a citric acid buffer was added and heated in a microwave oven to expose the antigenic sites. After being blocked, the sections were incubated with anti-MMP-9. The color development was performed with diaminobenzidine (DAB; MXB, China), images were observed with the ISC acquisition system, the positive area was calculated using Image-Pro Plus 6 image software.

2.7 Enzyme-linked immunosorbent assays (ELISA).

All mice were fasted for 12 hours and then given anesthesia (sodium 40mg/kg 1%), and 0.9 mL of blood was collected. In order to separate the serum, we centrifuged it at 3,000 rpm for 10 minutes at 4°C for 10 minutes . The concentrations of Triglyceride (TG), Low-Density Lipoprotein Cholesterol (LDL-C), High-Density Lipoprotein Cholesterol (HDL-C), TNF-α, and IL-1β in serums were determined by ELISA kits (Sinobestbio, Shanghai, CHINA) based on the manufacturer's instructions.

2.8 Quantitative real-time qRT-PCR

The total RNA was extracted from the carotid artery using TRIzol and reverse transcribed into cDNA with PrimeScript RT Master Mix. The primers sequences of NLRP3, ASC, Caspase-1, IL-1β, IL-18, ULK1, Beclin1, ATG7, LC3B, P62 are listed in Table 2. qRT-PCR was performed using SYBR Green PCR Master Mix and a Bio-Rad CFX96 Touch system (Bio-rad Laboratories, CA, USA).

2.9 Western Blot Analysis.

The total protein was extracted from carotid artery and cells. Measured protein concentration using BCA protein assay kit (Beyotime, Shanghai, China) and adjusted to the same concentration for each group of proteins. The equal volumes of protein samples were isolated by sodium dodecyl SDS-PAGE gel electrophoresis (Solarbio, Beijing, China). Then transferred to PVDF membranes (Roche, New York, USA) and blocked in 5% skim milk for 1h and then incubated with primary antibodies against NLPR3, ASC, Caspase-1, ULK1, MTOR, Phospho-MTOR, Beclin1, Atg7, LC3B, P62 (1:1000) and GAPDH (1:2500) overnight at 4°C. The membranes were incubated with the secondary antibody for 1h at room temperature, and immunoblot analysis and

quantification were performed with an iBrightä FL1000 instrument in the presence of an ECL kit (Beyotime, Shanghai, China).

2.10 Cells culture

RAW264.7 cells (Procell Life Science&Technology Co., Ltd.) were cultured with 37°C and 5% CO_2 in a cell incubator (ThermoFisher Scientific, MA, USA). Its medium was high-glucose Dulbecco's modified eagle medium (DMEM, Gibco, MA, USA) containing 10% fetal bovine serum (FBS, Clark Bioscience, Claymont, USA), 10 KU/L penicillin, and 10mg/L streptomycin (Gibco, MA, USA).

2.11 Cell Viability Assay

HJTF extract was freeze-dried and stored at -80°C. The RAW264.7 cells were added to 96-well plates with 1×10^5 cells/mL. The cells of each group were divided with the Blank group (without cells), DMSO group, Control group (without drugs), LPS group, and different concentrations of HJTF (0.25, 0.5, 1, 2, 4, 8, 16 mg/mL) groups. The Blank and Control group added 100ul DMEM medium. The DMSO group added DMEM medium containing DMSO (1μg/mL). Others added 100ul of DMEM medium containing LPS (1μg/mL) to each group. After 24 hours, the HJTF group was added with 100ul of HJTF medium of different concentrations (0.25, 0.5, 1, 2, 4, 8, 16 mg/mL). The Blank group, Control group, and the LPS group were added with 100ul of DMEM medium, and the DMSO group added DMEM medium containing DMSO (1μg/mL). After 24 hours of incubation, 10 μL of Cell Counting Kit-8 reagent (Boster Biological Technology, Wuhan, China) was added to each well and incubated with cells for about 1 h. Absorbance was measured at 450 nm using a microplate reader (Tecan, Switzerland).

2.12 Statistical Analysis.

All data were expressed as the mean ± S.D. One-way ANOVA was performed with Stata 25.0 (SPSS, Inc., Chicago, IL). Differences between groups were analyzed using Tukey's multiple comparison test. $P<0.05$ was considered a statistically significant difference.

3. RESULTS

3.1 The effect of HJTF on risk factors for atherosclerosis.

To determine the efficacy of HJTF on AS risk factors with mice, we gauged body weight and blood lipids in mice. As shown in Figures 2(A)-2(B), the bodyweight of the mice in the Model group gained obviously contrasted with the Sham group.

Subsequently, we used ELISA kits to detect the blood lipid in the serum of each group of mice. It showed that contrasted with the Sham group, TC and LDL-C in the serum of the Model group were obviously increased, but there was no apparent change in HDL-C. After administration of HJTF and Evolocumab, TC and LDL-C decreased significantly (Figures2(C)-2(E)). It can be considered that HJTF can reduce mice's weight and blood lipids to reduce atherosclerosis risk factors.

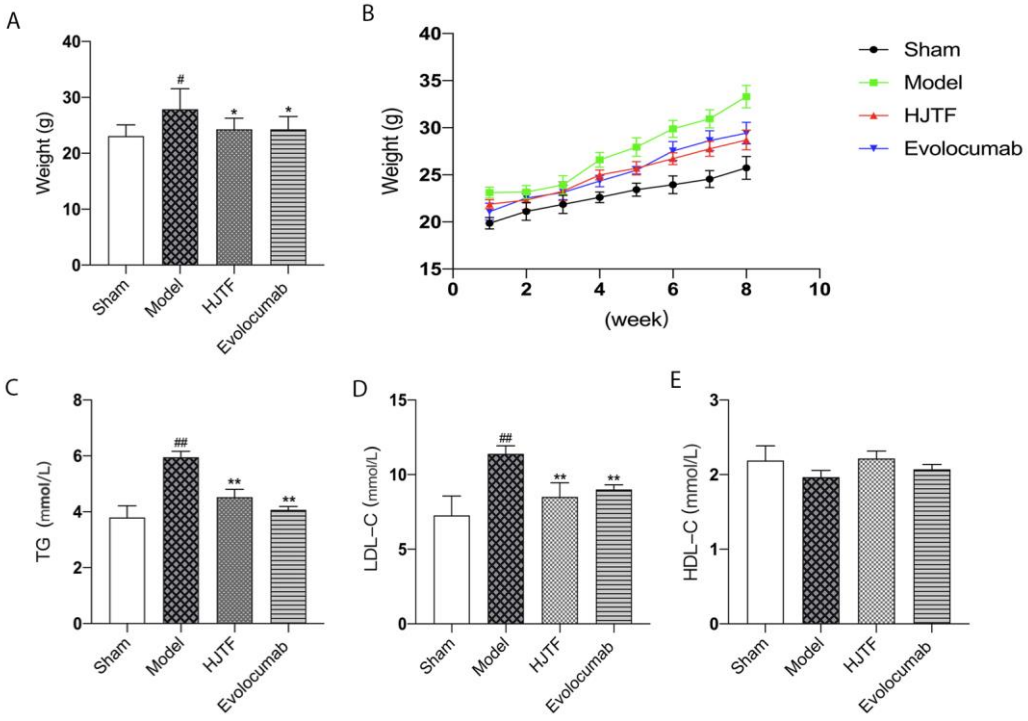

Figure 2. HJTF reduces AS risk factors in *ApoE*$^{-/-}$ mice. (A) Mean body weight of mice in each group. (B) Trends in body weight of mice in each group with feeding time. (C-E) ELISA kit examined the levels of TG, LDL-C, and HDL-C in the serum of each group of mice. Data were expressed as mean ± SD. (n=3). $^{\#}p<0.05$, $^{\#\#}p<0.01$, $^{\#\#\#}p<0.001$ vs. the Sham group, $^{*}p<0.05$ vs. the Model group, $^{**}p<0.01$, $^{***}p<0.001$ vs. the Model group

3.2 The effect of HJTF on carotid intima in ApoE$^{-/-}$ mice.

To the effect of HJTF on the intima with mice, we used histological assessment to examine the carotid arteries of each group of mice. H&E staining showed that the carotid artery in the Model group was clearly cramped and the intima was thicker than those in the Sham group. HJTF and Evolocumab alleviated endothelial hyperplasia and

increased the lumen area (Figure 3(A)-3(B)). Masson staining showed higher collagen attached in carotid arteries in the Model group than in the Sham group. Compared with the Model group, HJTF and Evolocumab reduced the percentage of carotid collagen deposition and fibrotic area (Figure 3(C)-3(D)). The results suggest that HJTF can inhibit intimal thickening, luminal stenosis and collagen fiber deposition in carotid arteries of ApoE$^{-/-}$ mice.

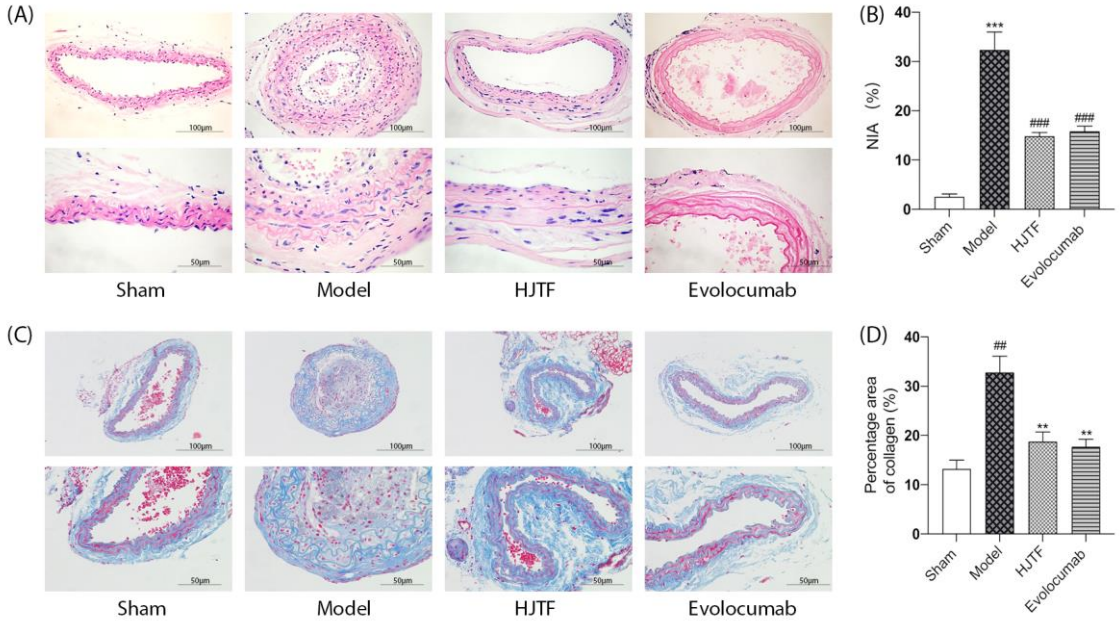

Figure 3. Histological assessment to examine the effect of HJTF on neointima formation and fibrosis in *ApoE*$^{-/-}$ mice. (A) HE staining was performed to assess the effect of HJTF on neointima of mice in each group (original magnification: 200× or 400×). (B) Average NIA ratio. (C) Masson staining of mice in each group was performed to evaluate the effect of HJTF on deposition and fibrosis (original magnification: 200×or 400×). (D) Percentage area of collagen. Data were expressed as mean ± SD. (n=3). $^{\#\#}p<0.01$, $^{\#\#\#}p<0.01$ vs. the Sham group, $^{**}p<0.01$, $^{***}p<0.001$ vs. the Model group.

3.3 HJTF regulated MMP-9 expression in the neointima of carotid arteries of ApoE$^{-/-}$ mice.

MMP-9 is a member of the matrix metalloproteinase subfamily, which has a significant role in degrading the extracellular matrix and causing fibrous cap thinning by degrading collagen fibers and connective tissue within the fibrous cap. High expression of MMP-9 can promote the development of VP. We used immunohistochemical methods to detect the regulation of HJTF on the expression of MMP-9 in the inner membrane of mice. The study suggested that comparison to the Sham group, the level of MMP-9 in the Model group was clearly increased, and the

content of MMP-9 was down-regulated after the administration of HJTF and Evolocumab, which was statistically significant comparison to the Model group. The same result was obtained by calculating the positive area (Figures 4(A)-4(B)). It is suggested that HJTF can reduce the MMP-9 in the plaque.

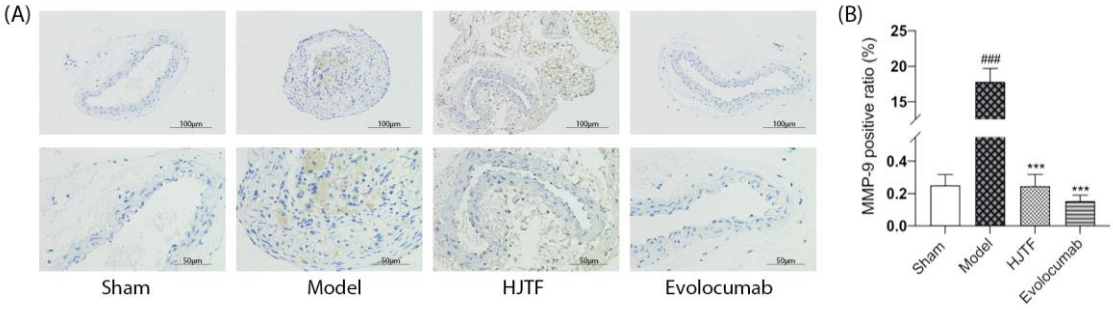

Figure 4. HJTF decreased MMP-9 expression in the carotid intima of *ApoE*$^{-/-}$ mice. (A) Representative images of immunohistochemical staining for MMP-9 in sections of the mice from each group (original magnification: 200×or 400×). (B) Percentage of MMP-9 positive area in each group. Data were expressed as mean ± SD. (n=3). $^{###}p < 0.001$ vs. the Sham group. $^{***}p<0.001$ vs. the Model group.

3.4 The effect of HJTF on NLRP3 Inflammasome in ApoE$^{-/-}$ mice carotid arteries.

Overexpression of NLRP3 inflammasome is one of the main factors in developing atherosclerotic VP. In this regard, we examined the expression of NLRP3 inflammasome in carotid arteries. The results showed NLRP3, ASC, Caspase-1, IL-1β, and TNF-α in the Model group were markedly increased. After the HJTF and Evoloumab, it decreased significantly (Figures 5(A)-5(J)). Meanwhile, ELISA suggested that IL-1β and TNF-α were considerably higher in the serum of mice in the Model group comparison to the Sham group, and significantly down-regulated in the HJTF and Evolocumab groups comparison to the Model group (Figures 5(K)-5(L)). These results indicated that HJTF can reduce the overexpression of NLRP3 inflammasome and inflammatory factors.

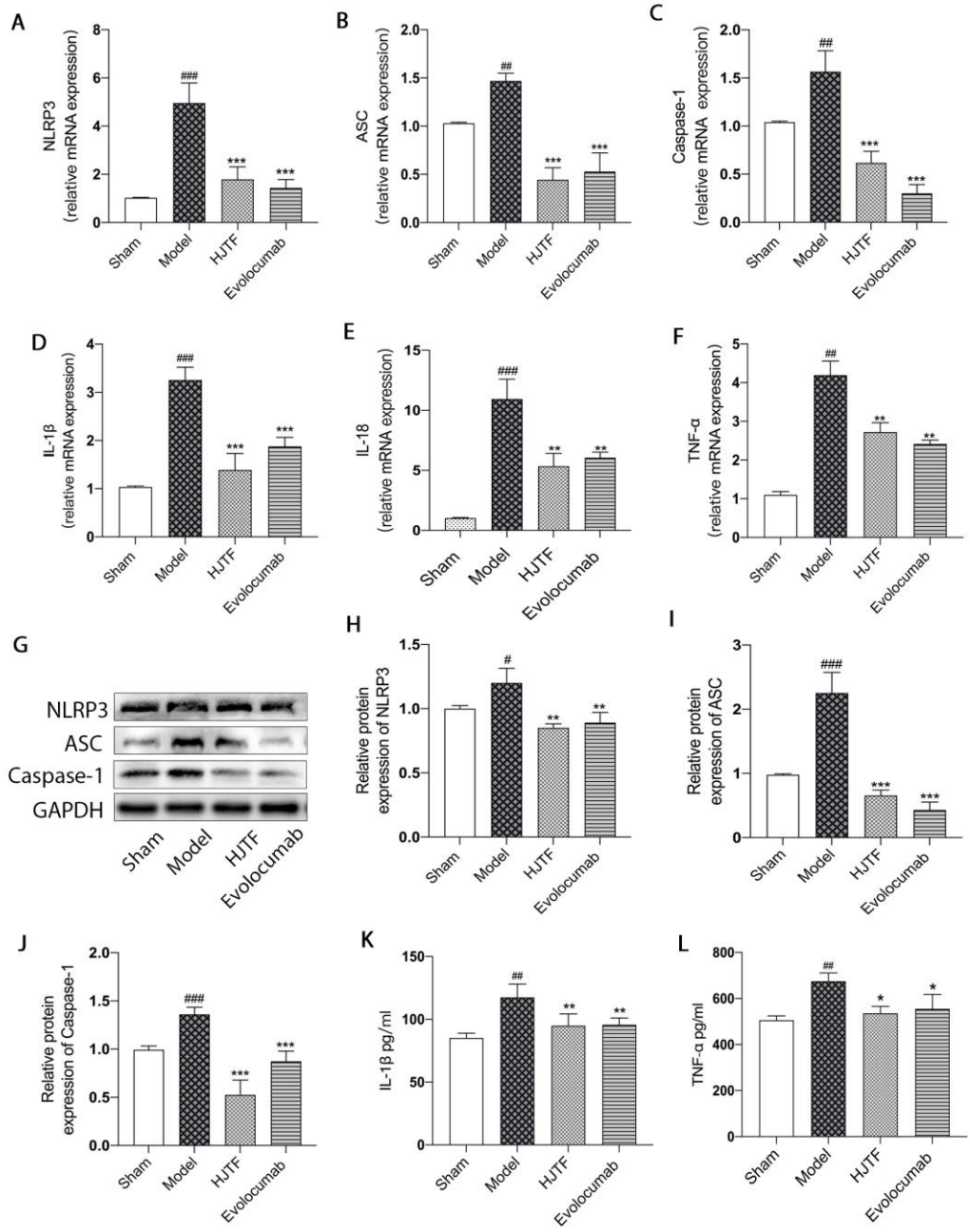

Figure 5. HJTF reduced excessive NLRP3 inflammasome expression in the carotid arteries of *ApoE*$^{-/-}$ mice. (A-F) RT-PCR detected the effect of HJTF on the mRNA expression of NLRP3, ASC, Caspase-1, IL-1β, IL-18, TNF-a in the Carotid artery of mice. (G-J) Western Blot assay the protein expression of NLRP3, ASC, Caspase-1 in Carotid artery of mice. (K-L) ELISA assay the expression of IL-1b and TNF-a in mice serum. Data were expressed as mean ± SD. (n=3). $^{\#}p < 0.05$, $^{\#\#}p < 0.01$, $^{\#\#\#}p < 0.001$ vs. the Sham group. $^{*}p < 0.05$,$^{**}p < 0.01$,$^{***}p < 0.001$ vs. the Model group.

3.5 Regulation of carotid artery autophagy levels in ApoE$^{-/-}$ mice by HJTF.

Autophagy is a "self-healing" process of the organism. Moderate autophagy can regulate excessive inflammatory responses in the organism. To clarify the regulation of

autophagy on NLRP3 inflammasome in mouse carotid arteries, we examined autophagy-related factors. The study showed that the level of ULK1 in the Model group was markedly lower than that in the Sham group (Figure 6(A) and Figure 6(F)). The phosphorylated mTOR was markedly higher than the Sham group, suggesting that autophagy received inhibition in the Model group during the initial stage of autophagy (Figure6(G) and Figure6(I)). We found that the expression of Beclin1, ATG7, and LC3B, a marker of autophagosome maturation, was significantly lower in the Model group, the level of autophagy was inhibited at the stage atherosclerotic VP. Therefore, we further investigated the changes in the expression of P62, a bridging protein between autophagy and inflammasomes. Free P62 was significantly elevated when autophagy was inhibited, suggesting that autophagy's recognition and degradation of inflammasomes were inhibited. HJTF and Evoloumab injection had a significant inhibitory effect on these phenomena. These data indicated that HJTF can regulate the autophagy-NLRP3 inflammasome signaling pathway.

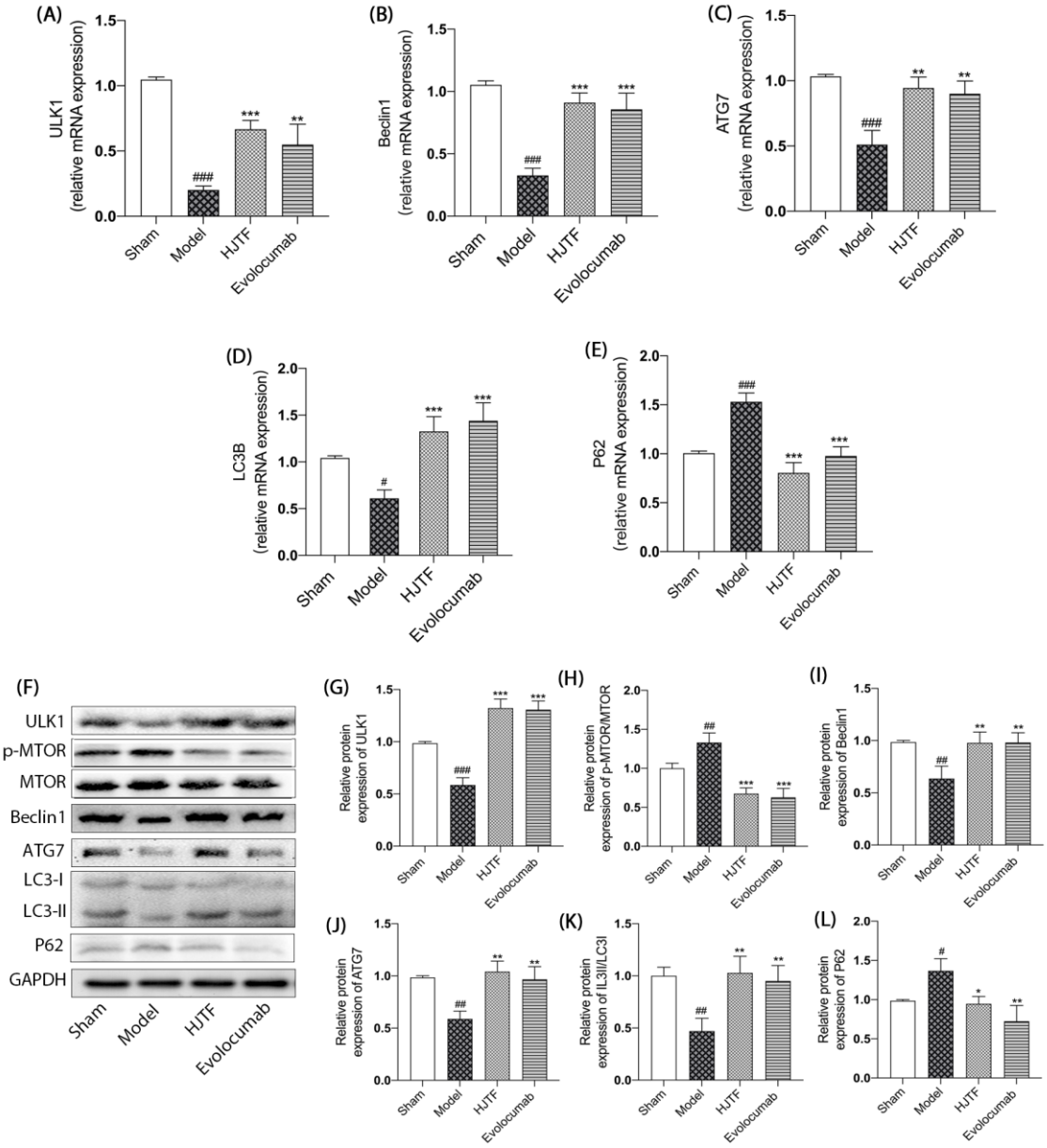

Figure 6. HJTF enhanced the level of autophagy in the carotid arteries of *ApoE*$^{-/-}$ mice. (A-E) RT-PCR detected the effect of HJTF on the mRNA expression of ULK1, Beclin1, ATG7, LC3B, P62. (F-K) Western Blot assay the effect of HJTF on the protein expression of ULK1, MTOR, Beclin1, ATG7, LC3B, P62. Data were expressed as mean ± SD. (n=3). $^{\#}p < 0.05$, $^{\#\#}p < 0.01$, $^{\#\#\#}p < 0.001$vs. the Sham group. $^{*}p<0.05$, $^{**}p < 0.01$,*** $p < 0.001$ vs. the Model group.

3.6 HJTF increased the activity of LPS-induced RAW264.7 cells.

To clarify the effect of HJTF on macrophage inflammatory injury, we used LPS to induce inflammatory injury in RAW264.7 cells and then gave varying degrees concentrations of HJTF and measured the cellular activity of each group using the CCK-8 kit. Figure 7 illustrated that the Cell viability increased dose-dependent in the HJTF treatment compared to the LPS group, reaching maximum activity at 1.6

mg/mL.This result clarifies the protective effect of HJTF on RAW264.7 cells. Therefore, this concentration was chosen for the subsequent experiments.

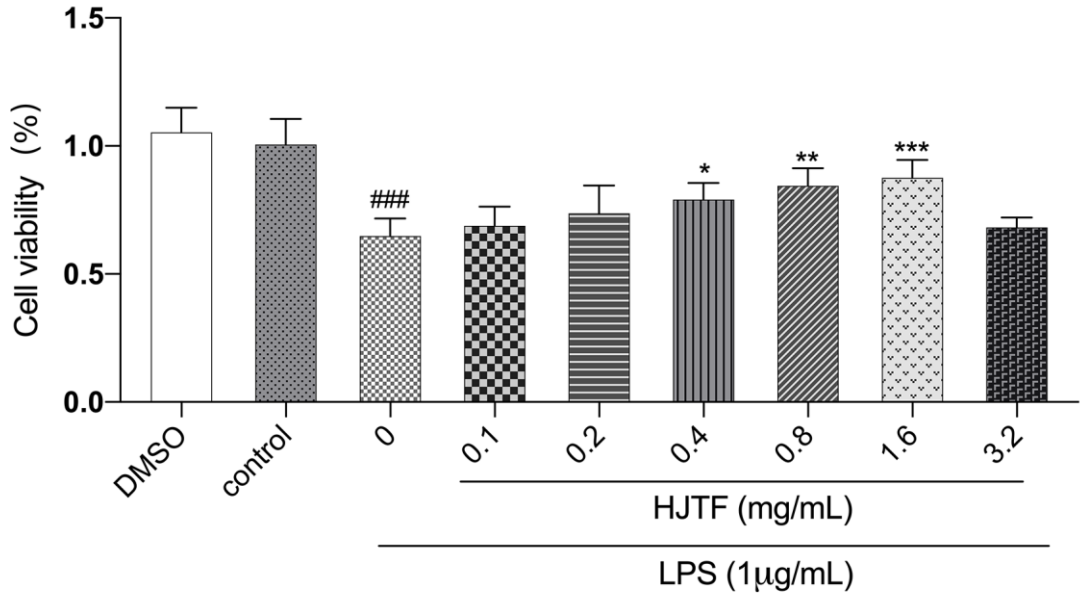

Figure 7. The effects of HJTF on RAW264.7 cells viability with the treatment of LPS-induced injury. Data were expressed as mean ± SD. (n=3). $^{###}p < 0.001$ vs. The Control group. $^{*}p<0.05$, $^{**}p < 0.01$, $^{**}p < 0.001$ vs. the LPS group.

3.7 HJTF Reduces Inflammatory Response by Regulating Autophagy Levels in RAW264.7 Cells

To further clarify the mechanism of the therapeutic effect of HJTF on RAW264.7 cells, we detected the expression levels of inflammation and autophagy in the cells by Western Blot. The results indicated that the NLRP3 inflammasome in the LPS group was markedly higher than those in the Control group, and the autophagy-related indexes decreased. After the administration of HJTF and Evolocumab injection, the inflammatory expression decreased and the autophagy level increased. Ubiquitinated protein P62 decreased (Figure (8)). It is suggested that HJTF and Evolocumab can improve LPS-induced macrophage damage through the autophagy-NLRP3 inflammasome signaling pathway.

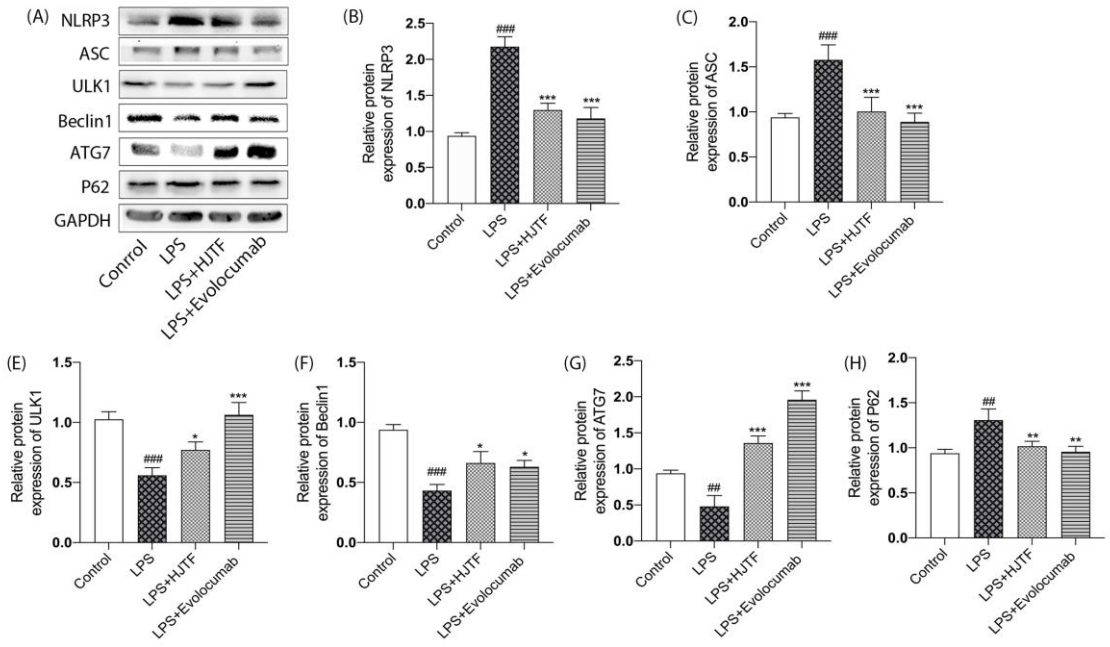

Figure 8.The effects to HJTF on Autophagy- NLRP3 Inflammasome Signal pathway after LPS-induced injury of RAW264.7 cells. Data were expressed as mean ± SD. (n=3). $^{\#}p < 0.05$, $^{\#\#}p < 0.01$, $^{\#\#\#}p < 0.001$ vs. The Control group. $^{*}p < 0.05$, $^{**}p < 0.01$, $^{***}p < 0.001$ vs. the LPS group. LPS group (LPS 1 μg/mL), LPS+HJTF group (LPS 1 μg/mL + HJTF 1.6 mg/mL), and LPS+Evolocumab group (LPS 1 μg/mL + Evolocumab 100 μg /mL)

4. DISCUSSION

The rupture of atherosclerotic VP can generate adverse cardiovascular events just like acute coronary syndrome. Plaque stabilization is the first choice to prevent the adverse consequences of VP. TCM is unique in its diagnostic and therapeutic guidelines and characteristics, and further research on TCM could provide viable approaches for preventing and treating VP.

HJTF has been shown to inhibit restenosis after coronary intervention by modulating ERS-autophagy signaling. Previous studies have clarified the main ingredients of the formula by HPLC-MS/MS and identified chlorogenic acid, tannic acid A, ferulic acid, tannic acid B, hapamid, tanshinons, and tanshinone glycyrrhizol side G2 in the formula, which provided the basis for this study (Tian, Yu et al. 2021) (STable1). HJTF has been widely used in the clinic, and its effect in treating VP is satisfactory, but its mechanism is not clear. Evolocumab is a novel lipid-lowering drug that suppress proprotein convertase subtilisinkexin type 9 (PCSK9). It can reduce the risk of adverse cardiovascular events by decreasing LDL-C levels (Sabatine, Giugliano et al. 2017). Thus, we used Evolocumab as a comparator drug in this study.

Obesity and hyperlipidemia are risk factors that promote the formation of AS. Effective suppression of AS risk factors can prevent and mitigate the occurrence and development of AS (Pierre Amarenco 2020). In this study, we found that the body weight of mice decreased after the administration of HJTF and Evolocumab. We also found that although there was no obvious difference in HDL-C of mice in each group, TC and LDL-C in both HJTF and Evolocumab groups were significantly reduced compasion with the Model group. It suggested that HJTF could reduce the risk factors of AS, such as obesity and hyperlipidemia. Meanwhile, histopathological results showed that HJTF inhibited endothelial proliferation and deposition of intravascular collagen fibers. Indicating it can inhibit luminal narrowing and suppress AS plaque formation. The above results predict that HJTF has a preventive effect on AS.

As one of the main components of the fibrous cap, the extracellular matrix plays an important factor keeping the stability of plaques. Matrix metalloproteinases (MMPs) can break down matrix components and promote cellular reabsorption of the matrix. They continuously accumulate in unstable plaques, leading to the degradation and destruction of blood vessels' extracellular matrix and increasing plaque instability (Brown, Williams et al. 2017, Johnson 2017). MMP-9 is a member of the matrix metalloproteinase subfamily, which has a significant role in degrading the extracellular matrix and causing thinning of the fibrous cap by degrading collagen fibers and connective tissue within the fibrous cap to form VP (Li, Li et al. 2020). Our study showed that the positive area of MMP-9 expression in the carotid arteries of mice in the Model group was significantly higher. The positive area of MMP-9 decreased after the administration of HJTF, suggesting that HJTF can reduce the expression of MMP-9 to stabilize plaques.

Inflammation is one of the main causative factors of VP (Back, Yurdagul et al. 2019). Nod-like receptor protein 3 (NLRP3) can be activated by cholesterol crystals, ox-LDL, and hemodynamic abnormalities, and recruit apoptosis-associated spot-like protein (SPECK-like protein, ASC) to activate the effector protein cysteine aspartic protein 1 precursor (pro-caspase-1), forming the NLRP3 protein complex and shearing activated caspase-1, the activated caspase-1 enzymes can split and activate IL-1β and IL-18 (Qiao, Ma et al. 2021). The NLRP3 inflammasome recognizes various inflammatory factors associated with AS, such as lipid crystallization(Cai, Wen et al. 2021). During the development of AS, cholesterol is mainly deposited in the intima, and

macrophages and endothelial cells can take up cholesterol and form cholesterol crystals, which can act as inflammatory factors that can further activate the NLRP3 inflammasome in macrophages and release IL-18 and IL-1β (Martinez, Celermajer et al. 2018). Among them, IL-1β can reactivate macrophages and lymphocytes and promote the release of other chemokines and inflammatory factors, resulting in the proliferation and migration of vascular smooth muscle cells (Lutgens, Atzler et al. 2019). When the inflammatory response occurs, it leads to apoptosis, the accumulation of cholesterol efflux in the apoptotic cells, and the cholesterol crystals inside and outside the cells can further activate macrophages, causing lysosomal rupture and oxidative stress, activating the NLRP3 inflammasome (Tall and Westerterp 2019). The above processes can cause adverse circulation and accelerate AS and even plaque rupture. This study found that the expression of the NLRP3 inflammasome-related indicators was markedly increased in the Model than in the Sham group. After HJTF gavaged, all inflammatory indicators decreased. These results suggest that HJTF reduces the inflammatory expression of atherosclerotic VP. It is necessary to conduct more studies to clarify the mechanisms that regulate the inflammatory response.

According to studies, proper activation of autophagy could regulate the NLRP3 inflammasome (Cosin-Roger, Simmen et al. 2017). During the initial phase in autophagy, the mammalian target of rapamycin (MTOR) can inhibit the activation of autophagy. When MTOR is inhibited, ULK1 activity is elevated and the ULK1-Atg13-FIP200 complex moves toward the endoplasmic reticulum region to form autophagic precursors. Beclin1 is a regulator of autophagosome formation and can recognize TRIF or MyD88 to inhibit the combination of Beclin1 and Bcl-2 and increase Beclin1, promoting autophagy. During the maturation phase of the autophagosome, LC3-I binds covalently to phosphatidylethanolamine and forms LC3II in the presence of ATG7. As a maker of autophagosome formation, LC3II is located in various parts of the autophagic membrane (Dikic and Elazar 2018).

One of the central pathways for substrate recognition and degradation by autophagy is ubiquitination. Ubiquitin chains can be selectively bound by the ubiquitin-binding domain (UBD) on proteasomes or autophagosomes, and the UBD can decode different ubiquitin chain types and structures, allowing substrate proteins connected to different ubiquitin chains to be selected explicitly for proteasomal or autophagic pathway degradation. p62/SQSTM1 is a selective autophagy receptor that contains an

N-terminal BP1 structural domain, an LIR motif, and a C-terminal UBA structural domain with ubiquitin binding. During autophagy, ubiquitin ligases tag inflammatory substrates via multiple Ub chains, bind Ub to the UBA structural domain in the p62/SQSTM1 protein ubiquitin binding-associated protein, them form a complex with LC3II to direct autophagy to identify substrates and remove them precisely.(Lamark, Svenning et al. 2017). In this process, LC3 binds to the bridging protein P62, enabling precise recognition of substrates by autophagy. When cellular autophagy is inhibited, accumulation of P62 often occurs (Jeong, Zhang et al. 2019). P62 acts as a bridging that recognizes the ASC subunit of the inflammasome and transfers it to the autophagosome for degradation. When autophagy is activated, the ASC subunit of the NLRP3 inflammasome is first labelled by ubiquitinated molecules. The P62 protein then recognizes the ubiquitinated tag and forms a complex. The P62 loaded with substrate recognizes the LC3 molecules on the autophagic vesicles and assembles, finally forming a substrate-ubiquitin molecule-P62 complex that is transferred to the autophagic vesicles for degradation (Jung Hwa Ko 2017). Ultimately, the autophagy's precise recognition and degradation of NLRP3 inflammasome were achieved through the autophagy-NLRP3 inflammasome signalling pathway. Our study found that when NLRP3 inflammasome was highly expressed in the Model group, the level of mTOR also increased. On contrast, the level of Beclin1, ATG7, LC3B, and other indicators were down-regulated. The expression of ubiquitinated molecule-free p62 was also increased, suggesting that the autophagy level of the organism was in a low state at this time. With HJTF, free P62 was reduced, autophagy-related indexes Beclin1, Atg7, and LC3B expression were increased, and NLRP3 inflammasome-related indexes were downregulated. Therefore, it is believed that HJTF may attenuate atherosclerosis and stabilize plaque through the autophagy-NLRP3 inflammasome signalling pathway.

Macrophages are typically inflammatory cells, with the highest levels of inflammatory cells in plaques (Xu, Jiang et al. 2019). They play a prominent element in the development of carotid AS plaques. When the endothelium is damaged to form AS plaques, the monocyte/macrophage system of the circulatory system is activated and recruited to migrate to the vessel wall. The inflammatory response is further amplified, increasing the risk of carotid plaque rupture (Z-J Shen 2018). To further elucidate the mechanism of HJTF regulation of atherosclerotic VP, we used LPS in vitro inflammation model experiments with mouse peritoneal macrophages RAW264.7. The

results showed that after LPS induced cells' inflammatory response, HJTF could improve cellular activity to a certain extent, reduce NLRP3 inflammasome vesicles and other related inflammatory responses, and improve the autonomy of macrophages autonomy phagocytosis to achieve cell protection.

5. CONCLUSION

In conclusion, our results confirm that HJTF effectively reduced proliferation and fibrosis of neointima in atherosclerotic VP model mice. It also inhibited the expression of MMP-9 in plaques. In addition, HJTF regulated the autophagy-NLRP3 inflammasome pathway and inhibited excessive inflammation in VP. In this study, we studied the mechanism of HJTF in treating VP. The treatment of VP with HJTF was explored from the perspective of autophagy and inflammation and provided the pharmacological basis for the clinical application of HJTF.

6. DATA AVAILABILITY STATEMENT

All data included in the article/supplementary information are directly inquired by the corresponding authors.

7. DISCLOSURE STATEMENT

The authors declare no conflicts of interest.

8. FUNDING

1.Science and Technology Research Plan Project of the Jilin Provincial Education Department of China (grant number. JJKH20210953KJ)
2.Natural Science Foundation of Jilin Province (grant number. YDZJ202201ZYTS159)
3.Natural Science Foundation of Jilin Province (General Project (Medical Science) grant number. YDZJ202301ZYTS204)

9. ABBREVIATIONS

AS: Atherosclerosis
ASC: acute coronary syndrome
HJTF: HuotanJiedu Tongluo Formula
HE: Hematoxylin-eosin

IHC: Immunohistochemistry

LPS: lipopolysaccharide

TNF-α: tumor necrosis factor-α

NLRP3: Nod-like receptor protein 3

ASC: apoptosis-associated spot-like protein

ox-LDL:oxidized low density lipoprotein

IL-1β: Interleukin-1β

IL-18: Interleukin-18

TCM: Traditional Chinese medicine

NIA: neointimal area

BSA: bovine serum albumin

MMP-9: matrix metalloprotein-9

TG: Triglyceride

LDL-C: Low-Density Lipoprotein Cholesterol

HDL-C: High-Density Lipoprotein Cholesterol

PCSK9: proprotein convertase subtilisinkexin type 9 (PCSK9)

ApoE: Apolipoprotein E

VLDL: very-low-density lipoprotein (VLDL)

FUNDING

1.Science and Technology Research Plan Project of the Jilin Provincial Education Department of China (grant number. JJKH20210953KJ).

2.Natural Science Foundation of Jilin Province (grant number. YDZJ202201ZYTS159).

3.Natural Science Foundation of Jilin Province (General Project (Medical Science) grant number. YDZJ202301ZYTS204).

REFERENCES

Back, M., A. Yurdagul, Jr., I. Tabas, K. Oorni and P. T. Kovanen (2019). "Inflammation and its resolution in atherosclerosis: mediators and therapeutic opportunities." Nat Rev Cardiol 16(7): 389-406.

Biasizzo, M. and N. Kopitar-Jerala (2020). "Interplay Between NLRP3 Inflammasome and Autophagy." Front Immunol 11: 591803.

Brown, B. A., H. Williams and S. J. George (2017). "Evidence for the Involvement of Matrix-Degrading Metalloproteinases (MMPs) in Atherosclerosis." Prog Mol Biol Transl Sci 147: 197-237.

Cai, Y., J. Wen, S. Ma, Z. Mai, Q. Zhan, Y. Wang, et al., (2021). "Huang-Lian-Jie-Du Decoction Attenuates Atherosclerosis and Increases Plaque Stability in High-Fat Diet-Induced ApoE(-/-) Mice by Inhibiting M1 Macrophage Polarization and Promoting M2 Macrophage Polarization." Front Physiol 12: 666449.

Cosin-Roger, J., S. Simmen, H. Melhem, K. Atrott, I. Frey-Wagner, M. Hausmann, et al., (2017). "Hypoxia ameliorates intestinal inflammation through NLRP3/mTOR downregulation and autophagy activation." Nat Commun 8(1): 98.

Dikic, I. and Z. Elazar (2018). "Mechanism and medical implications of mammalian autophagy." Nat Rev Mol Cell Biol 19(6): 349-364.

Elbialy, A. (2021). "In vivo autophagy quantification: Measuring LC3 and P62 puncta in 3D image system from zebrafish larvae." J Cell Biochem 122(10): 1435-1444.

Giuliani, C. (2019). "The Flavonoid Quercetin Induces AP-1 Activation in FRTL-5 Thyroid Cells." Antioxidants (Basel) 8(5).

Herrington, W., B. Lacey, P. Sherliker, J. Armitage and S. Lewington (2016). "Epidemiology of Atherosclerosis and the Potential to Reduce the Global Burden of Atherothrombotic Disease." Circ Res 118(4): 535-546.

Hettwer, J., J. Hinterdobler, B. Miritsch, M. A. Deutsch, X. Li, C. Mauersberger, A. Moggio, et al., (2021). "Interleukin-1beta suppression dampens inflammatory leukocyte production and uptake in atherosclerosis." Cardiovasc Res.cvab 337.

Hoseini, Z., F. Sepahvand, B. Rashidi, A. Sahebkar, A. Masoudifar and H. Mirzaei (2018). "NLRP3 inflammasome: Its regulation and involvement in atherosclerosis." J Cell Physiol 233(3): 2116-2132.

Huebbe, P. and G. Rimbach (2017). "Evolution of human apolipoprotein E (APOE) isoforms: Gene structure, protein function and interaction with dietary factors." Ageing Res Rev 37: 146-161.

Jeong, S. J., X. Zhang, A. Rodriguez-Velez, T. D. Evans and B. Razani (2019). "p62/SQSTM1 and Selective Autophagy in Cardiometabolic Diseases." Antioxid Redox Signal 31(6): 458-471.

Johnson, J. L. (2017). "Metalloproteinases in atherosclerosis." Eur J Pharmacol 816: 93-106.

Jung Hwa Ko, S.-O. Y., Hyun Ju Lee,Joo Youn Oh (2017). "Rapamycin regulates macrophage activation by inhibiting NLRP3 inflammasome-p38 MAPK-NFκB pathways in autophagy- and p62-dependent manners." Oncotarget 8(25): 40817-40831.

Kelley, N., D. Jeltema, Y. Duan and Y. He (2019). "The NLRP3 Inflammasome: An Overview of Mechanisms of Activation and Regulation." Int J Mol Sci 20(13).

Lamark, T., S. Svenning and T. Johansen (2017). "Regulation of selective autophagy: the p62/SQSTM1 paradigm." Essays Biochem 61(6): 609-624.

Li, T., X. Li, Y. Feng, G. Dong, Y. Wang and J. Yang (2020). "The Role of Matrix Metalloproteinase-9 in Atherosclerotic Plaque Instability." Mediators Inflamm 2020: 3872367.

Li, T., M. Safitri, K. Zhang, Y. Wang, L. Huang, Y. Zhu, et al., (2020). "Downregulation of G3BP2 reduces atherosclerotic lesions in ApoE(-/-) mice." Atherosclerosis 310: 64-74.

Lutgens, E., D. Atzler, Y. Doring, J. Duchene, S. Steffens and C. Weber (2019). "Immunotherapy for cardiovascular disease." Eur Heart J 40(48): 3937-3946.

Marais, A. D. (2019). "Apolipoprotein E in lipoprotein metabolism, health and cardiovascular disease." Pathology 51(2): 165-176.

Martinez, G. J., D. S. Celermajer and S. Patel (2018). "The NLRP3 inflammasome and the emerging role of colchicine to inhibit atherosclerosis-associated inflammation." Atherosclerosis 269: 262-271.

Moss, H. E., R. An, T. Nelson and K. Li (2019). "Risk of Atherosclerotic Cardiovascular Disease Among US Adults: Use of 1999-2014 NHANES Data." J Prim Prev 40(5): 569-573.

Pan, J., Y. Cai, M. Liu and Z. Li (2021). "Role of vascular smooth muscle cell phenotypic switching in plaque progression: A hybrid modeling study." J Theor Biol 526: 110794.

Pierre Amarenco, C. H., Julien Labreuche, Hugo Charles, Maurice Giroud, Elena Meseguer, et al., (2020). "Carotid Atherosclerosis Evolution When Targeting a Low-Density Lipoprotein Cholesterol Concentration <70 mg/dL After an Ischemic Stroke of Atherosclerotic Origin." Circulation 142(8): 748-757.

Qiao, L., J. Ma, Z. Zhang, W. Sui, C. Zhai, D. Xu, et al., (2021). "Deficient Chaperone-Mediated Autophagy Promotes Inflammation and Atherosclerosis." Circulation Research 129(12): 1141-1157.

Sabatine, M. S., R. P. Giugliano, A. C. Keech, N. Honarpour, S. D. Wiviott, S. A. Murphy, et al., Committee and Investigators (2017). "Evolocumab and Clinical Outcomes in Patients with Cardiovascular Disease." N Engl J Med 376(18): 1713-1722.

Tall, A. R. and M. Westerterp (2019). "Inflammasomes, neutrophil extracellular traps, and cholesterol." J Lipid Res 60(4): 721-727.

Tian, T., K. Yu, M. Zhang, X. Shao, L. Chang, R. Shi, et al., (2021). "Huotan Jiedu Tongluo Decoction Inhibits Balloon-Injury-Induced Carotid Artery Intimal Hyperplasia in the Rat through the PERK-eIF2alpha-ATF4 Pathway and Autophagy Mediation." Evid Based Complement Alternat Med 2021: 5536237.

Urbak, L., B. V. Sandholt, M. Graebe, L. E. Bang, H. Bundgaard and H. Sillesen (2020). "Patients with Unstable Atherosclerosis Have More Echolucent Carotid Plaques Compared with Stable Atherosclerotic Patients: A 3-D Ultrasound Study." Ultrasound Med Biol 46(9): 2164-2172.

von der Thüsen JH, v. B. T., Biessen EA (2001). "Induction of rapid atherogenesis by perivascular carotid collar placement in apolipoprotein E-deficient and low-density lipoprotein receptor-deficient mice." Circulation 103(8): 1164-1170.

Xu, H., J. Jiang, W. Chen, W. Li and Z. Chen (2019). "Vascular Macrophages in Atherosclerosis." J Immunol Res 2019: 4354786.

Z-J Shen, C.-S. X., Y-P Li,J Li,J-J Xu,P Xia (2018). "Telmisartan inhibits Ang II-induced MMP-9 expression in macrophages in stabilizing atheromatous plaque." Eur Rev Med Pharmacol Sci 22(22): 8004-8012.

Corresponding Author:

Keying Yu

Department of Cardiovascular, Affiliated Hospital of Changchun University of Chinese Medicine, Changchun, Jilin, China

E-mail：18684316613@163.com